Presentation of Short Term Scientific Missions Ancona (IT) – Nottingham (UK) in 2017

Visitor: Luca Bastianelli[1] Franco Moglie[1]
Host: Gabriele Gradoni[2,3], David Thomas[3]

[1]Department of Information Engineering, Università Politecnica delle Marche, Ancona, Italy.
[2]School of Mathematical Sciences, University of Nottingham, UK.
[3]The George Green Institute of Electromagnetics Research, University of Nottingham, UK.

ACCREDIT – IC1407

STSM from Ancona to Nottingham in 2017

List

- (Mar 13–31): **Luca Bastianelli**, “*Analysis of chaotic electromagnetic environments*”
  Reference Number: COST-STSM-IC1407-36889
- (Jul 7–15): **Franco Moglie**, “*Reverberation chamber simulation on high performance computers*”
  Reference Number: COST-STSM-IC1407-38300
- (Oct 9–21): **Luca Bastianelli**, “*Analysis of chaotic electromagnetic environments*”
  Reference Number: COST-STSM-IC1407-38975

Numerical Approach – FDTD Simulation

Unfavorable

- ⋆ High Q-factor implies very long time for simulations
- ⋆ Stirrer effects must be observed over a large number of positions
- ⋆ High powerful computers are required

Favorable

- ⋆ "Embarrassing parallel" structure
  - time domain (FDTD and FFT): each stirrer position can run on a different MPI process
  - frequency domain (statistic analysis): each frequency can run on a different MPI process
- ⋆ FDTD code is easily parallelizable with OpenMP or MPI

FDTD Simulation

Parameters

- ⋆ Investigated band: 0.2–2.0 GHz
- ⋆ Time step: 50 ps and cell size: 15 mm ($\lambda/10$ at 2.0 GHz)
- ⋆ FDTD grid: 401 $\times$ 268 $\times$ 168
- ⋆ Wall losses replaced by equivalent volumetric losses
- ⋆ We analyzed 256 stirrer positions

FDTD Simulation

Computing resource: CINECA Lenovo Adam Pass (MARCONI)

- Architecture: Intel OmniPath Cluster
- Processor Type: Intel Xeon Phi 7250 Knights Landing at 1.40 GHz
- Racks: 50
- Computing Nodes: 3 600
- Cores/Node: 68
- Computing Cores: 244 800
- RAM: 16 GB/node of MCDRAM and 96 GB/node of DDR4
- Internal Network: Intel OmniPath Architecture 2 : 1
- Disk Space: 17 PB (raw) of local storage
- Peak Performance: 11 PFlop/s
- Ranked at position 14 in the Top 500 list of November 2017

PRACE Project

Computing resources granted under a PRACE project

- ⋆ 15th Call for PRACE Project Access
- ⋆ Proposal ID: 2016143324
- ⋆ Project name: SREDIT – Simulations of Radiated Emissions in Densely Integrated Technologies
- ⋆ Participants: Ancona, Granada, Nottingham, York
- ⋆ Awarded resources: 12 353 536 core-hours
- ⋆ System: Marconi KNL (CINECA, Italy)
- ⋆ We plan to apply the Call 17 that should open the 7 March 2018

Structure of the results

IEC 61000-4-21 Standard method

$$\rho_i = \frac{\sum_{j=0}^{N-1} a_j a_{j+i}}{\sigma_{2a}}$$

Number of the uncorrelated chambers' states

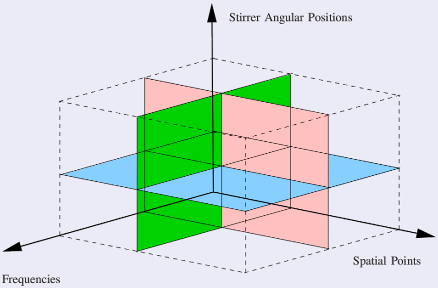

Evaluation of Uncorrelated frequencies

At each frequency step, the electric field values are computed in each point of a volumetric spatial grid

Multivariate approach

Matrix of the fields:

$$\underline{\underline{e}} = \begin{bmatrix} e_1^{(1)} & \dots & e_1^{(N_f)} \\ e_2^{(1)} & \dots & e_2^{(N_f)} \\ \vdots & \ddots & \vdots \\ e_{N_p}^{(1)} & \dots & e_{N_p}^{(N_f)} \end{bmatrix}$$

- ⋆ The columns are the field values at each frequency step
- ⋆ The rows are the field values in each spatial point

Multivariate Approach

Correlation matrix build up

ρ_{jk} is the Pearson correlation coefficient between the frequency points field arrays j and k for all the probed points

$$\underline{\underline{R}} = \begin{bmatrix} \rho_{11} & \rho_{12} & \cdots & \rho_{1N_f} \\ \rho_{21} & \rho_{22} & \cdots & \rho_{2N_f} \\ \vdots & \vdots & \ddots & \vdots \\ \rho_{N_f1} & \rho_{N_f2} & \cdots & \rho_{N_fN_f} \end{bmatrix} \qquad \rho_{jk} = \frac{\mathrm{Cov}\left(\underline{e}^{(j)}, \underline{e}^{(k)}\right)}{\sqrt{\mathrm{Var}\left(\underline{e}^{(j)}\right)\mathrm{Var}\left(\underline{e}^{(k)}\right)}}$$

- ⋆ Counting of uncorrelated frequency points using a threshold $[IEC\ 61000\ 4-21]$

$$N_u = \frac{N_f^2}{\#\left[\underline{\underline{R}} > r\right]}, \quad r = \frac{1}{e}\left[1 - \frac{7.22}{\left(N_f^2\right)^{0.64}}\right]$$

- ⋆ where r is the threshold value

Simulations

Simulated reverberation chamber

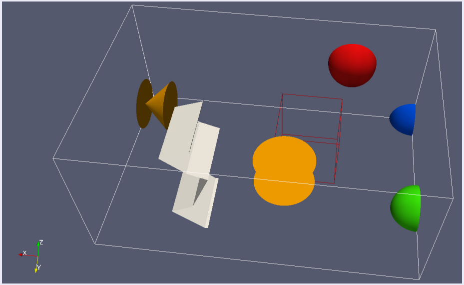

- Dimensions: $6 \times 4 \times 2.5$ m^3
- $f_0 \simeq 45$ MHz
- Discone antennas
- Curved diffractors
- Vertical stirrer
- Working volume

Simulations

Kind of diffractors

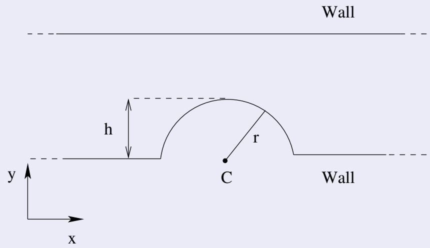

- r: radius
- C: center
- h: penetration
- h/r:
  - $=1$: hemisphere
  - <1: cap
  - >1: mushroom

Each configuration has a proper volume and surface correction

Simulations

Kind of diffractors

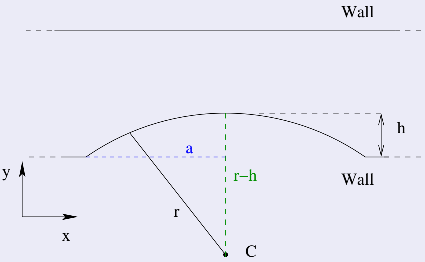

- r: radius
- C: center
- h: penetration
- h/r:
  - $= 1$: hemisphere
  - < 1: cap
  - > 1: mushroom

Each configuration has a proper volume and surface correction

Simulations

Kind of diffractors

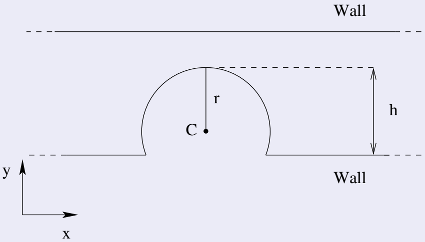

- r: radius
- C: center
- h: penetration
- h/r:
  - $=1$: hemisphere
  - <1: cap
  - >1: mushroom

Each configuration has a proper volume and surface correction

Results

Different kinds of diffractors on a corner

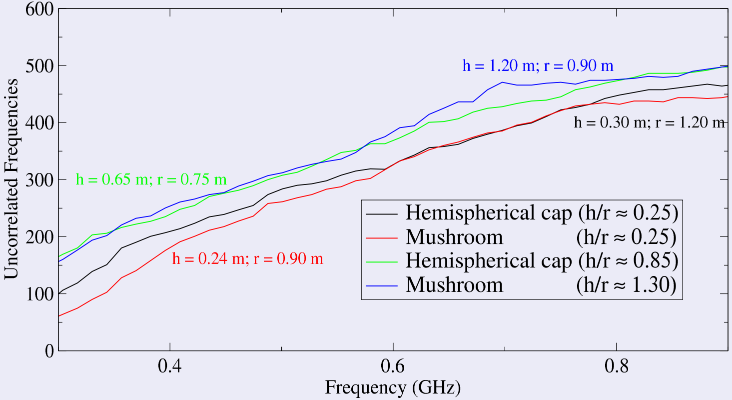

Quality factor

Q-factor of the cavity:

$$Q = \frac{16\pi^2 V \langle |S_{21}|^2 \rangle}{\eta_{TX}\eta_{RX}(1-|S_{11}|^2)(1-|S_{22}|^2)} \left(\frac{f}{c}\right)^3$$

For analytical analysis when wall losses are dominant, the Q-factor can be evaluated by:

$$Q_{ws} = \frac{3V^{ws}}{2\mu_r \delta S^{ws}} \; , \; Q_s = \frac{3V^s}{2\mu_r \delta S^s} \; ,$$

where $\delta = \frac{3}{\sqrt{\omega\mu\sigma}}$ is the skin depth [m]

The total volume and surface including diffractors are:

$$V^s = V^{ws} - \alpha \frac{4}{3}\pi r^3 \; [\text{m}^3]$$

$$S^s = S^{ws} + \beta\pi r^2 \; [\text{m}^2]$$

α and β depend on the number and position of diffractors

Simulations

Losses

Losses mechanism of antennas is given by:

$$Q_a = \frac{16\pi^2 V}{\lambda^3} \text{ (dominant at low frequency)}$$

then

$$Q_{tot}^{-1} = Q^{-1} + Q_a^{-1}$$

- Losses adopted within the theoretical model is $\sigma = 5000$ S/m
- Volumetric losses adopted in the FDTD is:
  - $\sigma_v = 1 \cdot 10^{-5}$ S/m for the empty chamber
  - scaled σ_v for a chamber loaded by spheres

Simulations

Modal overlap

- The average modal overlap is defined by:

$$M(f) = m(f)\frac{f}{Q(f)}$$

  $m(f)$ is the average modal density predicted by the Weyl's law

- The internal power transmission is evaluated by:
  $P(f) = \frac{\langle |S_{21}|^2 \rangle}{\eta_{Tx}\eta_{Rx}(1-|S_{11}|^2)(1-|S_{22}|^2)}$

- The modal overlap can be re-write as:

$$M(f) = \frac{8\pi V}{Q(f)}\frac{f^3}{c^3}$$

  by using the $P(f)$ is it possible to define an estimator:

$$\bar{M} = \frac{1}{2\pi P(f)}$$

  The $\bar{M}$ estimator does not require a-priori information about the cavity

Simulations

Label ID	#Spheres	r (m)	#1/8	#1/4	#1/2	V^s (m^3)	S^s (m^2)
Empty RC	0	//	//	//	//	60.0	98.00
A)	4	0.50	0	0	4	58.95	101.14
B)	10	0.50	2	4	4	58.29	102.31
C)	20	0.50	1	17	2	56.65	107.80
D)	30	0.50	4	18	8	55.45	110.50
E)	10	0.75	2	4	4	54.25	107.71

Simulations

Quality factor

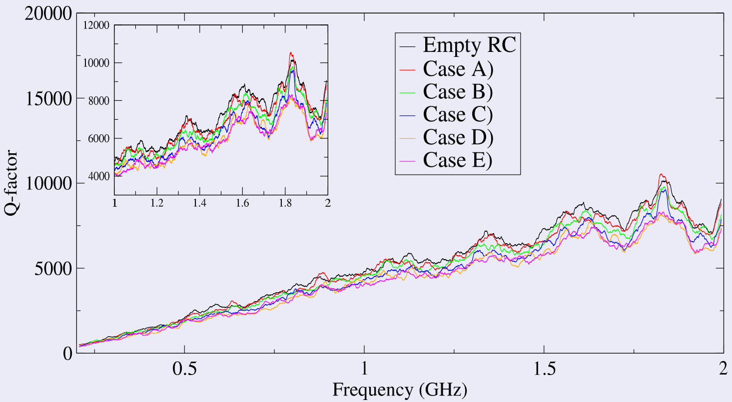

Simulations

Internal power transmission

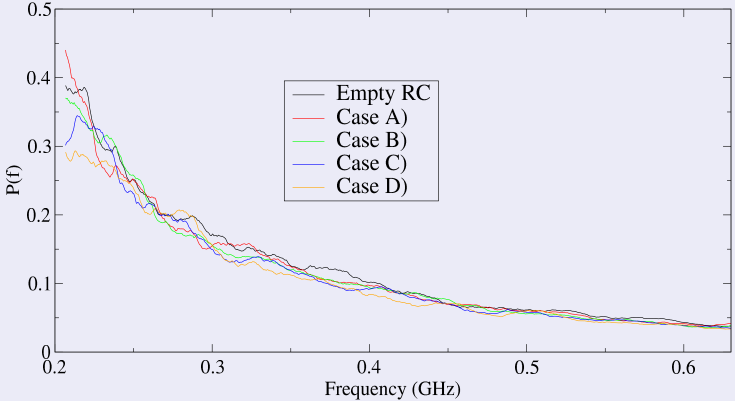

Simulations

Simulated vs estimated modal overlap

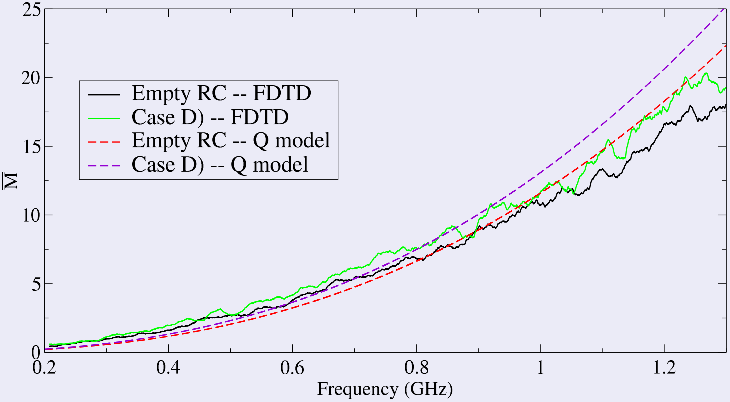

Simulations

Uncorrelated stirrer positions

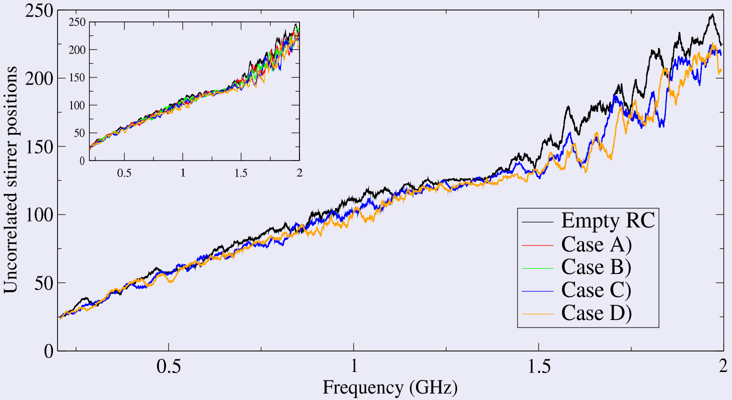

Simulations

Field uniformity – σ_{24}

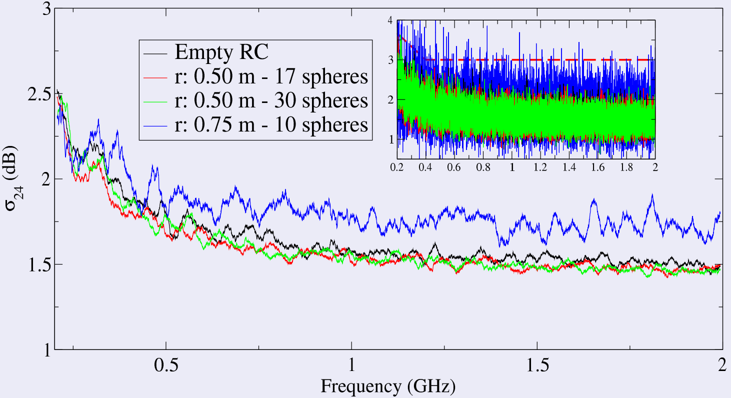

Simulations

Modal densities ratio as function of number of spheres

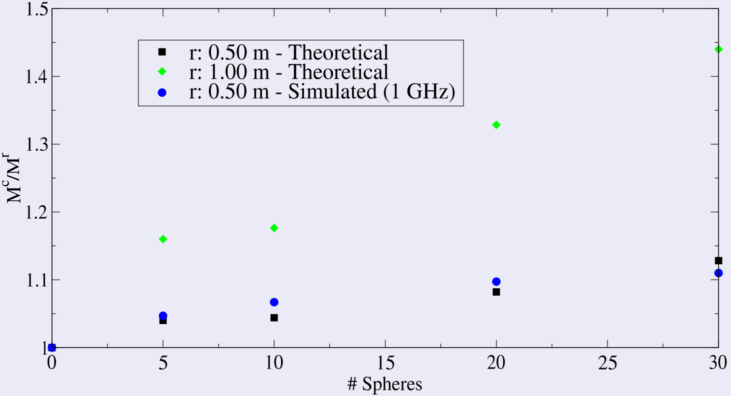

Experimental setup

Nottingham's RC

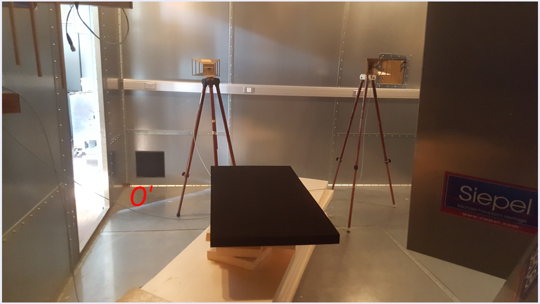

RC for emulation of real-life wireless environments

$$PDP(t) = \left\langle |h(t)|^2 \right\rangle_N \,, h(t) = \mathrm{IFT}[S_{21}]$$

$$\tau_{\mathrm{RMS}} = \frac{\sqrt{\int_0^\infty (t-\tau_{ave})^2 PDP(t)dt}}{\int_0^\infty PDP(t)dt}$$

$$\tau_{ave} = \frac{\int_0^\infty t\mathrm{PDP}(t)dt}{\int_0^\infty \mathrm{PDP}(t)dt}$$

In order to match the required time delay spread:

- ⋆ Tuning the PDP by adding absorbing material
- ⋆ Optimization of absorbing positioning

Typical Environments

Delay spread (ns)	NLOS Lab	LOS Lab	NLOS Room	LOS Room
Average	93.35	42.09	66.05	38.26
RMS	766.07	395.66	674.46	274.52
Average threshold -30 dB [1]	72.68	36.16	50.75	30.83
RMS threshold -30 dB [1]	34.25	22.54	30.46	20.64

Scenario		Delay spread (ns)
Indoor Hotspot	LOS	20
	NLOS	39
Urban Micro	LOS	65
	NLOS	129
	O-to-I	49
Suburban Macro	LOS	59
	NLOS	75
Urban Macro	LOS	93
	NLOS	365
Rural Macro	LOS	32
	NLOS	37

[1] Genender, E.; Holloway C.L.; Remley K.A.; Ladbury J.; Koepke G.; Garbe H., Use of reverberation chamber to simulate the power delay profile of a wireless environment, Int. Symp. Electromagn. Compat. - EMC Europe, Hamburg, Sep. 2008, pp. 1-6.

ITU Report M.2135-1, Dec. 2009

Results

Uncorrelated stirrer positions

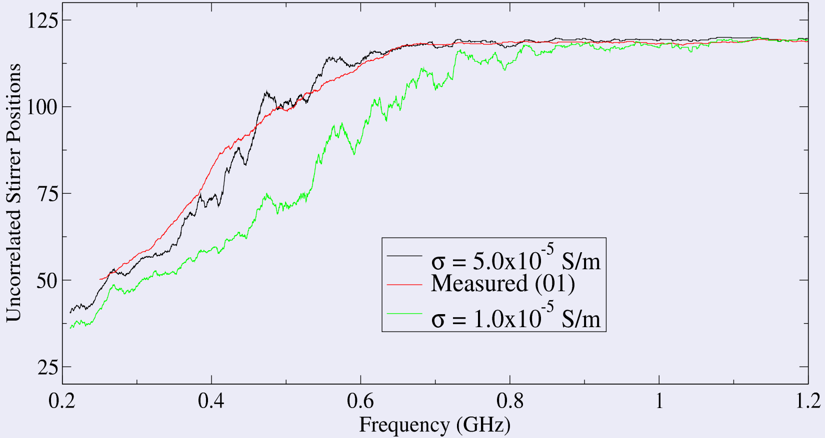

Absorbers

Measurements and simulations for a single absorber

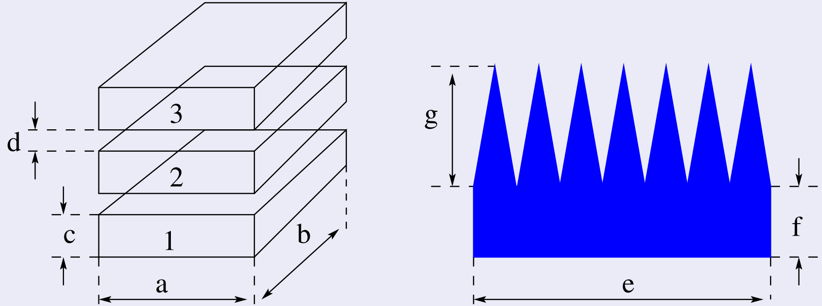

Layer number	1	2	3
ϵ_r (VHP-8)	1.2	1.5	1.7
σ (S/m) (VHP-8)	0.01	0.05	0.08

Results

Q-factor

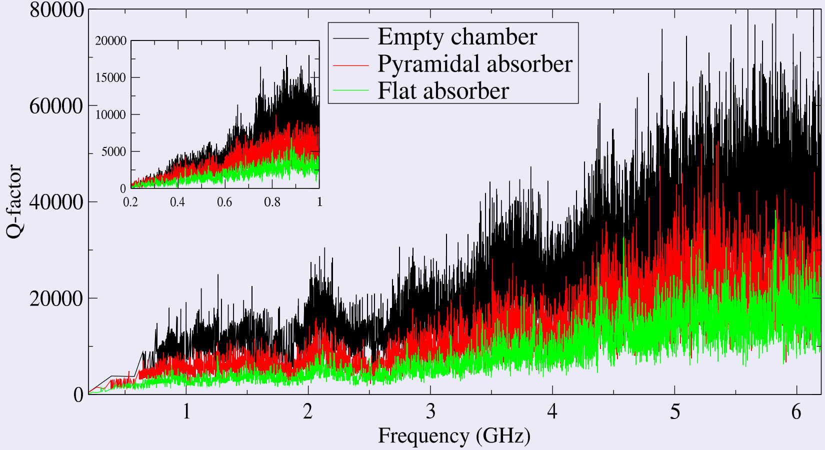

Results

Power delay profile

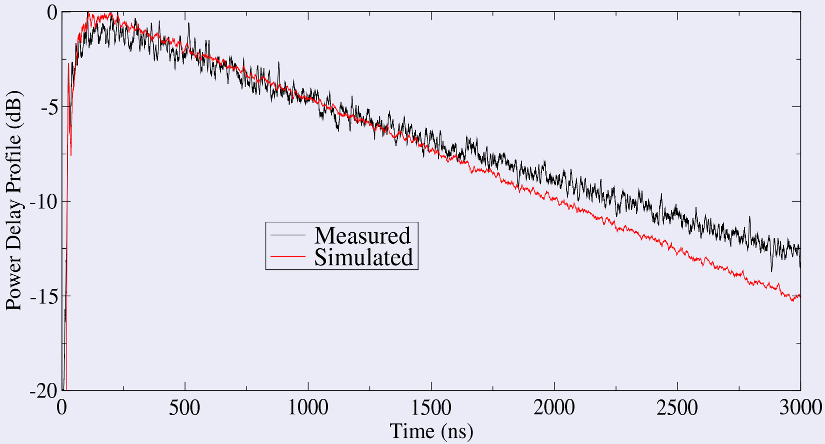

Publications

Conference Papers

- ⋆ L. Bastianelli, F. Moglie, V. Mariani Primiani, “*Evaluation of Stirrer Efficiency Varying the Volume of the Reverberation Chamber*” – EMCS 2016 Ottawa
- ⋆ L. Bastianelli, V. Mariani Primiani, F. Moglie, “*Effect of Loss Distribution on Uncorrelated Spatial Points and Frequency Steps in Reverberation Chambers*” – 2016 EMC EUROPE Wroclaw
- ⋆ L. Bastianelli, G. Gradoni, F. Moglie, V. Mariani Primiani, “*Full Wave Analysis of Chaotic Reverberation Chambers*” – URSI GASS 2017 – URSI Young Scientist Award Commission E
- ⋆ G. Gradoni, L. Bastianelli, V. Mariani Primiani, F. Moglie, “*Chaos Enhancement in Reverberation Chambers*” – European Microwave Week 2017
- ⋆ L. Bastianelli, G. Gradoni, F. Moglie, V. Mariani Primiani, “*Reverberation Chambers Deformed by Spherical Diffractors*” – EMC EUROPE 2017

Publications

Ph.D. Thesis

- Luca Bastianelli "*Analysis of Complex and Chaotic Electromagnetic Structures: the Reverberation Chamber and its Applications*" – To be defended in March 2018

Journal Paper approaching to submission:

- Chaotic Reverberation Chamber: Improving its Performance by Appropriate Boundary Deformations
- Evaluation of the Reverberation Chamber Time Constant From Power Delay Profile and σ

Conclusions

Measurements and Simulations of Nottingham Facilities

- ⋆ Comparison between FDTD simulation and experimental results
- ⋆ Loss effects
- ⋆ Best load configuration for wireless tests – Power delay profile and time delay spread

Diffusors improve the chamber's performance

- ⋆ Increase the radius
- ⋆ Increase the number of diffractors
- ⋆ Placement of diffractors is relevant
- ⋆ Choose the optimal diffractor
- ⋆ Trade off: performance/usable volume

Conclusions

Measurements and Simulations of Nottingham Facilities

- ⋆ Comparison between FDTD simulation and experimental results
- ⋆ Loss effects
- ⋆ Best load configuration for wireless tests – Power delay profile and time delay spread

Diffusors improve the chamber's performance

- ⋆ Increase the radius
- ⋆ Increase the number of diffractors
- ⋆ Placement of diffractors is relevant
- ⋆ Choose the optimal diffractor
- ⋆ Trade off: performance/usable volume